

RESEARCH ARTICLE

Reconfigurable fully constrained cable-driven parallel mechanism for avoiding collision between cables with human

Elham Khoshbin^{1,2,*} , Khaled Youssef¹, Ramy Meziane^{1,2} and Martin J.-D. Otis¹

¹LAR.i Lab, Applied Science Department, University of Québec at Chicoutimi, Québec, G7H 2B1, Canada and ²ITMI (Technological Institute of Industrial Maintenance), Sept-îles College, Sept-Îles, G4R 5B7, Canada

*Corresponding author. E-mail: elham.khoshbin1@uqac.ca

Received: 28 October 2021; **Revised:** 9 May 2022; **Accepted:** 17 June 2022; **First published online:** 1 September 2022

Keywords: cable-driven parallel mechanism, Karush–Kuhn–Tucker, collision avoidance, reconfiguration, workspace

Abstract

Productivity can be increased by manipulators tracking the desired trajectory with some constraints. Humans as moving obstacles in a shared workspace are one of the most challenging problems for cable-driven parallel mechanisms (CDPMs) that are considered in this research. One of the essential primary issues in CDPM is collision avoidance among cables and humans in the shared workspace. This paper presents a model and simulation of a reconfigurable, fully constrained CDPM enabling detection and avoidance of cable–human collision. In this method, unlike conventional CDPMs where the attachment points are fixed, the attachment points on the rails can be moved (up and down on their rails), and then the geometric configuration is adapted. Karush–Kuhn–Tucker method is proposed, which focuses on estimating the shortest distance among moving obstacles (human limbs) and all cables. When cable and limbs are close to colliding, the new idea of reconfiguration is presented by moving the cable’s attachment point on the rail to increase the distance between the cables and human limbs while they are both moving. Also, the trajectory of the end effector remains unchanged. Some simulation results of reconfiguration theory as a new approach are shown for the eight-cable-driven parallel manipulator, including the workspace boundary variation. The proposed method could find a collision-free predefined path, according to the simulation results.

1. Introduction

Industry 5.0 is introduced by the European Commission 10 years after the introduction of Industry 4.0. Industry 4.0 is discussed as technology-driven, while Industry 5.0 is presented as value-driven as it suggests bringing back humans in production [1]. Accordingly, Industry 5.0 brings the human touch with semi-autonomous robots inside a hybrid workspace in a mass product personalization concept. Using the intelligence of humans combined with tireless robots, flexible manufacturing could be adapted and upgraded for a mass (product) personalization which is limited in Industry 4.0 concepts. In this perspective, robots and humans will work together in same workspace. Humans focus on more complex tasks needing interpretation and robots do repetitive tasks. In human–robot co-working (such as physical cooperation, interaction, and task sharing), when humans and robots need to work in a same workspace, preventing human–robot collisions is an important and fundamental issue. Avoiding human–robot collisions in a shared workspace is the main topic of this paper such as discussed in ref. [2].

The SPADER project (Sharing Production Activities in Dynamic Environment) [3], presented as a new concept for Industry 5.0, could be applicable for cable-driven parallel mechanism (CDPM). CDPM consists of several components: a fixed base, an end effector, and m -cables to connect the base to end effector by set of pulleys and actuators. Compared to serial mechanisms, there are advantages for CDPM such as a large workspace and high dynamic. Also, CDPMs can be used to move or lift heavy objects in the industry [4], as haptic interfaces [5] and high-speed manipulators [6]. CDPMs are useful for

applications with high dynamic and velocity demands. High dynamic significantly increases the inertial effects of the moving end effector and must be considered in the end effector wrench computation. A controller can generate appropriate cable tension distribution for given end effector trajectories.

Researchers, active in the CDPM field, have been investigating on many challenges, such as dynamic trajectory planning [7] and control [8]. In the fully constrained CDPM, each wrench applied on the end effector can be balanced by pulling each cable with a tensile force control [9]. Moreover, the end effector can be moved in some poses (positions and orientations) due to the control of cables length [10], and all degrees of freedom of the end effector can be controlled through the cables.

However, to constrain the end effector, the number of cables (m) should be greater than the number of degrees of freedom (DOF) or $m \geq \text{DOF} + 1$. Given the above facts, wrench-closure workspace (WCW) is introduced as a set of a feasible pose of the end effector balanced through positive tension in the cables. The WCW is dependent on the geometry of the mechanism [11, 12]. On the other hand, if $m \leq \text{DOF}$, then the mechanism is known as under-constrained.

As an example of cable behaviors, the mass and elasticity of cables impact on the position accuracy of the end effector as suggested in refs. [13–15]. Moreover, in addition to cables mass and elasticity, sagging and vibration explored in refs. [16, 17] increase the cable length and then the position accuracy. In these studies, the cables are introduced by an elastic catenary. Considering the model of cables makes the system more complex for the position/velocity control, some papers assumed cables as massless inextensible lines [18] connecting the attachment points on the pulley with the end effector [19].

Cables are wound around a pulley to release or retract the cable through actuators. Pott [20] discussed the influence of a pulley in the winch. However, only a few authors have addressed the influence of pulleys (by modeling a pulley) on the kinematics [20] and dynamic simulation of CDPM [21].

In SPADER projects, the collaboration between humans and robots is required to achieve high-performance control and sensing so that operators can share the same workspace with robots. There is some traditional solution to ensure user safety by isolating the robot by fences or laser curtains. These solutions stop the robot immediately when it is very close to a human and avoid any risk of collision, limiting the task's flexibility. So, these methods are not applicable where humans and robots collaborate in the same physical workspace. The robots should respond accurately to human actions to have safe interaction in a shared workspace. In some applications where humans and robots are working in the same workspace, robots should track the predefined trajectory and perform some tasks such as assembly processes where the contact between humans and robots can be dangerous for humans. Whereas in CDPM mechanism, cables are hanging through the workspace, they can easily interfere with end effector, obstacles such as human limbs and other cables as mentioned by Nguyen and Gouttefarde [22]. Interference among cables and limbs could distort the whole end effector trajectory and cause a quick tension drift on the cables. Collision avoidance methods have been well studied for the case of serial and parallel robots. However, it is not well developed in the case of CDPM.

Makino et al. [23] designed a 6-DOF CDPM with eight cables using a rotational mechanism inside the end effector. Meanwhile, when a collision among cables is detected, control of cables is proposed by rotating the end effector around the vertical axis to change the configurations of the cables.

Lahouar et al. [24] adapt path planning method for cable robots that were developed for serial manipulators. Path planning is used when the robot is closed to an obstacle. An algorithm is used to detect the collision between the robot and the obstacle and between the cable and obstacle. This approach is used to find a free collision path in CDPM, whereas in the presented paper, we present a method to track predefined trajectory as a duplicated process. The most proposed approaches focus on finding a free collision path in CDPM. Still, these methods are not applicable for some processes where the trajectory is predefined and should not be changed, such as the assembly process. Reconfiguration of CDPM's components, such as motorized reels, may improve the capability of CDPM and increase the workspace size [25].

Workspace presented by Trautwein [26] is used to determine the geometry of cable-driven parallel robots. The theoretical kinematics of CDPM and reconfiguration CDPM is proposed. Analyzing workspace by considering the collision avoidance among cables or obstacles is not presented. Whereast

to avoid collision and track the predefined trajectory, the adaption of components positions or the workspace of the CDPM as geometric reconfiguration theory is proposed.

Gagliardini et al. [25] focuses on relocation of attachment points on the base of Reconfigurable Cable Driven Parallel Mechanism or RCDPMs. According to the environment, the designer divides the defined workspace in n parts. Trying to predict the collision between cables and object in the workspace can be used to divide the workspace. Each part can be covered and represented by just one configuration. So, for each configuration, the designer defines the set of possible locations for attachment points. By placing the attachment points on the possible locations, many CDPM configurations can be generated. There are set of constraints such as interference between cables and wrench feasibility. So, some configurations satisfying the constraints are selected. Combination of these configuration is needed to optimize presented objective functions to maximize productivity and minimize reconfiguration time. The reconfiguration process in 10 steps is explained in ref. [25]. To pass from one configuration to another, one or more cables must be disconnected from their initial attachment points and connected to new attachment points location. New attachment points position for all the configurations can be computed by an optimization algorithm to satisfy a set of constraints that are defined by the designer. This proposed method is used to reduce computational time, but it needs the knowledge of designer about trajectory to divide the workspace in n parts.

Xu and Park [27] used rapidly exploring random tree (RRT) method to address moving cube obstacle avoidance. The Gilbert–Johnson–Keerthi (GJK) algorithm is used to detect collision. In ref. [28], presented by Farzaneh Kaloorazi et al., obstacles are considered as a circle- (planar case) or spherical (spatial case)-shaped, and interference with limbs and end effector edges are discussed. Obstacle-free workspace of two parallel manipulators (a 3-RPR PM and 6-DOF Gough–Stewart) introduced an interval-based methodology. Meanwhile, this methodology is known as a computationally intensive approach due to the limitation of interval analysis. It causes high computing time in a high-degree equations.

Youssef and Otis [29] introduced an algorithm to prevent the collision between cables, whereas the trajectory of the end effector is unchanged. An algorithm is used to detect the contact between the two cables and which cables are in a higher position. So, it moves up the attachment points to increase the distance between the two cables to the safest threshold. In fact, first, the length of the cable and the pose of the end effector are determined, and second, distance between the cables are defined. If the distance between the two cables is less than the tolerance, the cable tension is computed, and finally, an increment on the attachment points is obtained.

This paper aims to model and analyze the reconfiguration of a 6-DOF parallel mechanism driven by eight cables to avoid collisions among cables and human limbs in the shared workspace. In this paper, a fully constrained CDPM can be introduced when the attachment points on the rails move vertically up and down. The length of cables can be modified according to the relocation of attachment points. The contribution of this paper is the collision avoidance among cables and human limbs (such as a moving obstacle in a dynamic workspace) in CDPM using Karush–Kuhn–Tucker (KKT) method. This idea applies by moving the linear displacement of attachment points on the rails to increase the shortest distance between cables and human limbs to a safe distance. This distance is computed by the KKT method as a collision detection algorithm. So, this algorithm can detect obstacles as quickly as possible. After distance detection, the algorithm moves reels or attachment points on the rails while keeping the desired trajectory of the end effector unchanged. Workspace analysis for all poses of the end effector is one of the important issues in designing CDPM. The effect of relocating the attachment points on the wrench feasible workspace of CDPM is presented, and then the feasible workspace was mapped for any change in the attachment points on rails. Section 2 is a review of previous research on technologies for collision avoidance in CDPM. In Section 3, a model of a 6-DOF mechanism driven by eight cables, given that the attachment points on the rails move vertically up and down, is presented. Sections 3.5 and 3.6 present the main contributions of this paper: the new reconfiguration is proposed to avoid collision among cables and human limbs by relocating attachment points on the rails. Also, KKT method is presented to compute the shortest distance between human limbs and cables while keeping the end

effector trajectory unchanged. Section 4 presents the differences between original and final workspaces and discusses the performance of the proposed method for a circular trajectory. Section 5 discusses the limitation of this study. Some related works in the same criteria of this paper are discussed in the next section.

2. Related work

2.1 Non-reconfigurable CDDM

The CDDM faces some constraints because cables can pull the end effector, not push it [24]. Merlet and Daney [30] indicates that collision between the cables and the end effector may limit the workspace. Nguyen and Gouttefarde [22] discussed that a collision may occur in some cases: (1) between cables, (2) between cables and the end effector (self-collision), (3) between the end effector and the environment, and (4) between cables and objects in the environment. In these situations, designing an algorithm to determine optimal trajectory motion between two collision-free configurations is important because the CDDM cables may collide with other cables, human, or static objects in the workspace.

Kowalczyk et al. [31] presented a vector field orientation control algorithm for the end effector in an environment with obstacles in order to track the desired trajectory. Also, the local artificial potential function (APF) [32] is used as a collision avoidance method that surrounds obstacles. So, a robot can be repulsed when it is close to the boundaries of obstacles. In the artificial potential field method, by defining the functions of artificial attraction and repulsion potential, the robot is attracted to the target and repelled by obstacles. Lyapunov function candidate is used to analyze stability. Lahouar et al. [24] worked on collision-free path planning for four-cable-driven parallel robot in order to avoid collisions between cables and obstacle and between cables.

There are some approaches in order to solve the path planning problem such as moving obstacles include APF methods [33], sample-based methods [34], geometry-based methods [35], and velocity obstacle-based methods [36]. Bak et al. [37] presented a modified goal-biased RRT algorithm and GJK algorithm to find the distance between the robot and fixed objects and solve the cable collision problem. Zhang et al. [38] proposed an improved RRT algorithm with a cost function in order to guarantee the obstacle avoidance and finding the optimal path. Bordalba et al. [39] proposed a method in order to find a collision-free path between two points while keeping the cables in tension and simultaneously adhering to the actuators and joints force capabilities. They validated their presented method by experimental data on a specific CDDM. Also, in the proposed method, positions and velocities of two points are needed to compute a collision-free path. A new method presented by Wischnitzer et al. [40] allows collisions between cables by expanding the workspace compared to free-collision workspace mechanisms. The presented method formulates the inverse kinematics of 6-DOF redundant CDDM by considering two colliding cables while keeping a feasible and positive WCW. They presented theoretical and experimental results and expansion workspace compared with a free-collision one. However, the vibration problem due to colliding cables, especially in high-speed applications, is not studied. Also, the friction at the contact point between cables is not considered. Aref and Taghirad [41] studied the collisions between cables, cable to the body of 6-DOF cable-driven manipulator. The whole workspace could be indicated based on designing a full force feasible mechanism, and then the workspace boundaries are recognized by a collision-free algorithm. Analysis of this approach takes less computational time and is practical in real-time application, while the collision between cables and obstacles inside the CDDM workspace is not considered, whereas the effect of the collision avoidance method in the workspace is discussed in our presented paper. Pinto et al. [42] proposed SPIDERobot as 4-DOF-driven mechanism for pick and place in industrial applications. A new approach is introduced based on visually locating the robot's position and the position of obstacles to optimize the robot's trajectory by visual interpretation of the workspace. This method can be helpful for collision avoidance between cables and the environment. Simulated models indicate that this approach is valid for cable mechanisms under constrain. However, this approach is not applied for reconfigurable, fully constrained CDDM. The authors do not present an analysis of the wrench or feasible workspace.

Wang et al. [43] presented the WCW of planar 3-DOF cable robot without collision. This research finds the area where the end effector and obstacles are not colliding. The study did not evaluate workspace and the performance of the method on different spatial geometric configurations (motorized reel location) of the CDPM. Blanchet and Merlet [44] investigated interference detection between the cable–cable and cable–objects for a 6-DOF freedom cable-driven robot by two algorithms based on interval analysis. The authors proposed a non-crossed cable model. The crossed cable configuration has a larger workspace and higher torques than the non-crossed cable configuration.

Otis et al. [45] proposed a method to manage cable interference between two 6-DOF foot platforms in a cable-driven locomotion interface. This method estimates the cable interference geometrically for any constrained trajectory. Then, they proposed an algorithm that could determine which cable could be released from an active actuation state while keeping cables in tension to maintain the trajectory. The problem of tension discontinuity is solved by presenting a collision prediction scheme applied to redundant actuators. Also, the limitation of the workspace as the main issue due to folding two cables on each other is discussed. This workspace is limited due to one cable release of its actuation state. A sudden increase in tension of other cables may cause mechanical vibration and instability.

More recently, Meziane et al. [46] proposed a new approach in order to avoid collision between cables by using an admittance controller when a robot is in physical interaction with a human. Collision detection between two cables can cause changing the trajectory of the end effector. While moving the end effector toward a collision, the user feels a virtual force and pushes the end effector to increase the distance between the two cables but in the inverse direction of the current motion to avoid this collision.

These previously studied algorithms implemented with fixed configurations on CDPMs affected the performance of the system to avoid collision with obstacles. Also, these algorithms for complex tasks and cluttered environments are not very reliable because the geometric configurations of CDPMs are limited. Indeed, reconfiguration is introduced by relocating the positions of the attachment points on base (motorized reel location) to allow the initial desired trajectory.

2.2 Geometric reconfiguration of the base

Variable-structure CDPMs can be defined by allowing collisions between cables and fixed objects in the workspace. Allowing collisions along the length of cables is discussed by Rushton and Khajepour [47]. Attachment points of cables can be changed when a collision is recognized along the length of a cable and cause changes in the dynamic structure of the mechanism. One of the significant advantages of variable-structure cable robot (VSCM) is the ability to cover a non-convex workspace. In comparison, moving obstacle is not discussed in this paper. Geometric reconfiguration method, proposed by Youssef and Otis [29], allows avoiding collision between cables by relocating attachment points on rails. However, collision avoidance method between cable and moving obstacles is not presented by authors. Anson et al. [48] investigated to add a moving base for a planar 3-DOF mechanism driven by four cables. Using mobile base for the CDPM increases kinematic redundancy which maximizes the size and quality of the WCW, but it requires precision to control.

A Tension Factor index tests the quality of the WCW. Also, the WCW is analyzed by comparing two planar mobile base configurations and a traditional CDPM. Two configurations, rectangular base and circular base, are introduced. Each base is restricted from moving on its linear rail in the rectangular configuration, and an angle is made between each rail and the two adjacent rails. Also, the bases are restricted from moving along a circular rail in a circular configuration. The authors mentioned that the circular base has a better WCW where the end effector could reach any position and orientation. This research focuses on planar CDPM, and cable interference avoidance is not presented.

2.3 Geometric reconfiguration of the end effector

Barbazza et al. [49] proposed a method as online reconfiguration of attachment points on the end effector for a 3-DOF under-constrained suspended CDPM with four cables. The reconfigurable end effector is

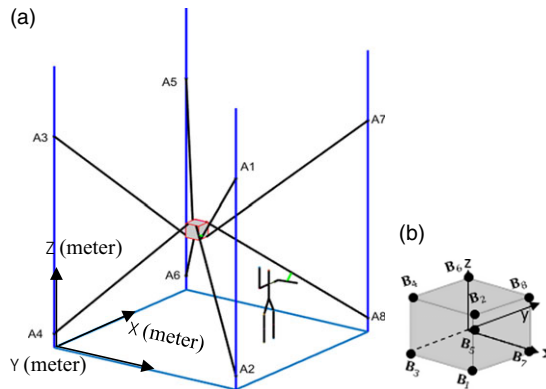


Figure 1. Geometric configuration of the cable-driven parallel mechanism: (a) Arrangement of attachment points on the rails and (b) arrangement of attachment points on the end effector.

presented by changing attachment points' position at the end effector to avoid collisions with obstacles. Also, when the end effector is far from obstacles, the attachment points on the end effector can be reconfigured to increase performance. The algorithm can be defined to optimize trajectory in some processes, such as pick and place. But in this research, attachment points on the base are fixed, and analysis workspace caused by online reconfiguration is not evaluated.

2.4 The perspective of this article

The initial trajectory in the haptic system or collaborative physical human–robot interaction should be unchanged because the trajectory comes from an operator. Still, the collision between cables and obstacles constrains the performance of CDPM and can be dangerous for user safety. This paper focuses on the collision avoidance method to improve the performance of CDPM using geometric reconfiguration with workspace analysis. Whereas the workspace between humans and robots is shared, previous research adapts the end effector's trajectory to avoid collision between cables or between cables and the environment or release a cable from its actuation state to keep the same trajectory. Some methods presented in previous section are used to track predetermined trajectory. Also, collision between cables and cables with obstacles are considered, whereas these methods may limit the workspace.

This paper presents a new method to detect and avoid collision between cables and human, while the trajectory of the end effector is unchanged and end effector tracks the trajectory inside the workspace. To perform this idea, a model of the interference between cables and human should be considered that is presented in Section 3.

3. Modeling the interference between cables and human

This section presents coordinate configuration and reconfiguration theory for the fully constrained CDPM. Modelling analysis of CDPM by symbolically establishing the coordinate system is then discussed. As a contribution to this paper, a new method based on the KKT condition to compute the distance between all cables and human limbs is proposed. Finally, the relocation of corresponding attachment points on the fixed frame is presented.

3.1 Coordinate system and attachment points

In this study, a fixed global frame (X – Y – Z) can be seen in Fig. 1, at the bottom left corner, and the Z axis direction is vertically upward, and the X – Y axes can be found according to right-hand rule. Whereas

Table I. Initial positions of the eight attachment points (m).

	A_1	A_2	A_3	A_4	A_5	A_6	A_7	A_8
X	0	0	0	0	7	7	7	7
Y	0	0	7	7	7	7	0	0
Z	7.5	0.5	7.5	0.5	7.5	0.5	7.5	0.5

Table II. Local positions of the eight attachment points (m).

	B_1	B_2	B_3	B_4	B_5	B_6	B_7	B_8
X	-0.15	-0.25	-0.15	-0.25	0.15	0.25	0.15	0.25
Y	-0.25	-0.15	0.25	0.15	0.25	0.15	-0.25	-0.15
Z	-0.25	0.25	-0.25	0.25	-0.25	0.25	-0.25	0.25

Table III. Human limbs length (m).

Human height	2.2
Arm length	0.5
Leg length	1.2
hand length	0.25

the attachment points on the rails are fixed in conventional CDPM, to avoid collision, our approach moves up/down the cable attachment points on the rail (reel location) in order to increase the distance between the human with cables to the safest threshold as suggested in ref. [50]. As it can be observed in Fig. 1, servo-actuated reels are connected to the moving platform with eight cables to get a fully constrained CDPM in the six DOFs. Each cable is connected to the end effector at points B_i . To relocate the attachment points on rails A_i , equations are obtained to find the desired cable length to reach a given end effector position and orientation. Suggested configuration is used to detect distance between cables and human and to obtain new position of attachment points on rails while keeping the end effector trajectory unchanged. In this research, the cables are considered massless and straight lines.

To verify the performance of the presented approach to avoid collision between cables and a human in the shared workspace, a human skeleton is inserted through a colliding distance with cables in simulation where the end effector performs its trajectories for its production tasks.

There are eight attachment points (B_i) on the end effector (rectangular prism shape). The dimensions of the end effector are $0.5 \times 0.5 \times 0.5 \text{ m}^3$. The location of attachment points (A_i) on the base and the locations of the attachment points (B_i) on the end effector with respect to the local frame (ε in meters) are observed respectively in Table I and Table II.

The human limbs length and human height are presented in Table III.

Kinematic and driving constraints are discussed in Sections 3.2 and 3.3. These constraints should be considered to evaluate forward and inverse kinematics. Kinematic constraint restricts moving attachment points only in vertical direction.

3.2 Kinematics constraints

The generalized coordinates of the system or \vec{q} consisting of \vec{q}_{ac} and \vec{q}_{er} are presented in (1):

- (a) \vec{q}_{ac} is defined as generalized coordinates of the attachment points on the rail.

(b) \vec{q}_{er} is defined as generalized coordinates of the attachment points on the end effector.

$$\begin{aligned} \vec{q} &= \left[(\vec{q}_{er})^T, (\vec{q}_{ac})^T \right] \\ \vec{q}_{er} &= [X_p, Y_p, Z_p, \alpha_p, \beta_p, \gamma_p], \\ \vec{q}_{ac} &= [X_i, Y_i, Z_i] \end{aligned} \tag{1}$$

In this project, the movement in vertical direction is limited for each attachment points. Kinematic constraints for moving in X and Y directions have been restricted as follows [29]:

$$\begin{bmatrix} x_i \\ y_i \end{bmatrix} = \begin{pmatrix} k_i^1 \\ k_i^2 \end{pmatrix} \quad i = 1 \text{ to } n \tag{2}$$

Cartesian coordinates of attachment points on reels in the global coordinate system are indicated by x_i and y_i . k_i is a constant and indicates attachment points position with respect to the fixed frame.

3.3 Driving constraints

The driving constraints are introduced as defined motion trajectories. In this project, three groups of driving constraints are considered.

- a. The first group of driving constraints, due to the vertical motion of the eight attachment points on the rails, is presented in (3) as suggested in ref. [29]:

$$z_i = c_i(t, \vec{q}) \quad \text{for } i = 1 \text{ to } n, \tag{3}$$

where z_i is defined as Z coordinate of each reel on the rails and $c_i(t, \vec{q})$ is a function to drive the attachment point vertically. Also, this function should depend on t (time), \vec{q} (generalized coordinates), human limbs velocity, and sampling frequency for example.

For this research work, this value is fixed as a constant. Therefore, each attachment point can move vertically 0.1 m up and down in simulation as explained in Section 3.6.

- b. The second group of driving constraints can be introduced due to the extension and retraction of each cable attached to the end effector. It is indicated by changing the length of cables. The length of the cable can be defined by hypotenuse of a right-angle triangle by the vertices A_i , B_1 , and B_{1z} . As can be seen in Fig. 2, these equations of second group constraint are presented as follows:

$$(\mathbf{B}_x)_i^2 + (\mathbf{B}_y)_i^2 + (\mathbf{A}_i - (\mathbf{B}_z)_i)^2 = p_i^2 \quad \text{for } i = 1 \text{ to } n \tag{4}$$

- c. The third group of driving constraints in this paper is workspace analysis. Workspace analysis of CDPM is the ability of the end effector to translate or orient under some constraints. Five workspace categories are introduced: static equilibrium workspace, WCW, feasible wrench workspace, dynamic workspace, and collision-free workspace [51]. The feasible wrench workspace is presented as all possible positions and orientations of the end effector while maintaining a positive tension among all the cables. Set of positive tension vector in all the cables maintain each set of external wrenches acting on the end effector. The feasible wrench workspace is presented as follows:

$$\vec{w}\vec{t} + \vec{w}_j = \vec{0}_6 \quad t_{min} < \vec{t} < t_{max} \quad \text{and} \quad \vec{w} = \begin{bmatrix} \vec{u}_1 & \dots & \vec{u}_8 \\ \vec{r}_1\vec{u}_1 & \dots & \vec{r}_8\vec{u}_8 \end{bmatrix} \tag{5}$$

\vec{w}_j or external wrench acting on the end effector is weight of the end effector as 25 n in the Z direction. \vec{w} and \vec{t} are structure matrix and tension in the cables, respectively. The two variables (\vec{r}_i and \vec{u}_i) in the structure matrix \vec{w} are explicit functions in the position and orientation of the end

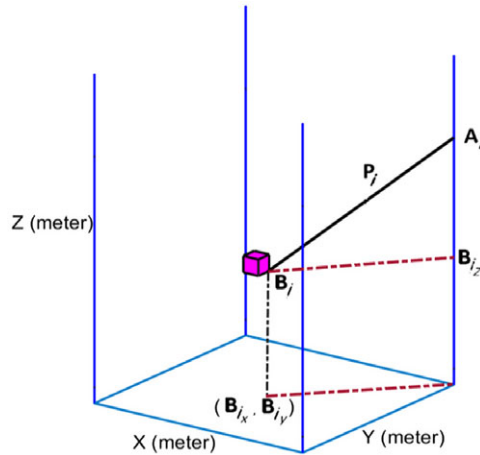


Figure 2. Second group of driving constraints [29].

effector as well as the attachments points position. The tension of each cable is positive value, and it is between minimum tension $t_{min} = 20$ and maximum tension $t_{max} = 90$ n [29].

Finally, the total constraint equations can be introduced as Eqs. (2) to (5). The next section presents the algorithm to solve the forward and inverse kinematics using these constraints.

3.4 Forward and inverse kinematic of proposed reconfiguration theory

3.4.1 Forward kinematic

In conventional CDPM, the forward kinematics is used to manipulate and control the position and orientation of the end effector as output given the cable lengths. However, in the reconfigurable CDPM, the forward kinematic algorithm is evaluated to compute cartesian coordinates of the reference frame of the end effector given the linear displacement of attachment points on rails $c_i(t, \vec{q})$ and the eight cable lengths as inputs [29]. The Levenberg–Marquardt least squares method [52] is used to solve the forward kinematics problem.

3.4.2 Inverse kinematic

Figure 3 shows the schematic for the end effector and attachment points A_i , where O is the fixed global frame and ε is a local frame attached to the end effector. This figure shows cable i and human limb as two-lines segments.

In the reconfigurable CDPM theory proposed in this paper, the inverse kinematics is defined as (5). Meanwhile, that variable inputs are introduced as the pose of the end effector and the attachment point’s location on the reels, and output is known as cable length. Regarding Fig. 3, the vector loop-closure equation or length of cables for cable i is introduced as follows:

$$p_i = \|\vec{B}_i - \vec{r}_{A_i}\| \text{ for } i = 1 \text{ to } n \tag{6}$$

where (7) indicates the coordinates of point B_i as follows:

$$\vec{B}_i = \vec{r}_{ef} + R\vec{r}'_i \text{ for } i = 1 \text{ to } n \text{ (number of cables)} \tag{7}$$

\vec{r}_{ef} is the position vector of the center of mass of the end effector and R is introduced as rotation matrix of moving platform frame with respect to local frame. \vec{r}'_i is the local coordinate frame attached to the end effector ε . Shortest distance computation can be used to detect collision between human and cables that is discussed in next section.

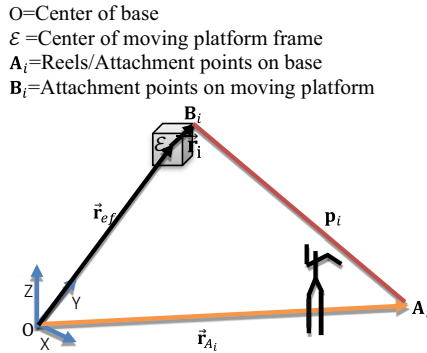


Figure 3. Second group of driving constraints.

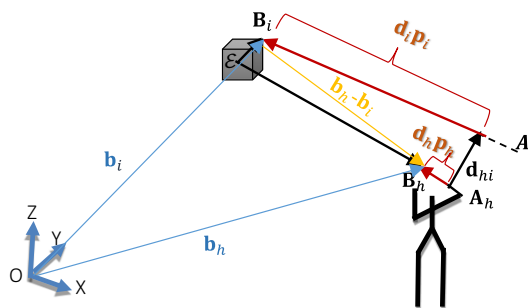


Figure 4. Vector formulation of the distance between limb and cables.

3.5 Shortest distance computation as collision detection between cables and human

Some formulations are introduced to define the interference contact points [53]. One method is based on determining a line perpendicular to two lines to define the shortest distance. Whereas interference happens when the cables are coplanar, it is necessary to add a condition to recognize that an intersection occurs inside or outside the cable lengths. The shortest distance between cables can be geometrically computed as discussed in refs. [46] and [53]. Two non-dimensional variables \mathbf{d}_h and \mathbf{d}_i are introduced, where $\mathbf{d}_i \mathbf{p}_i$ and $\mathbf{d}_h \mathbf{p}_h$ are illustrated by red lines in Fig. 4. $A_i B_i$ and $A_h B_h$ present the length of eight cables and human arm, respectively. $\mathbf{d}_i \mathbf{p}_i$ is distance between B_i and the line that represents the shortest distance between cable and human. $\mathbf{d}_h \mathbf{p}_h$ is distance between B_h and the line that represents the shortest distance between cable and human. This new approach is used to avoid cables being parallel at infinity. \mathbf{d}_{hi} is introduced as a distance vector between cables and human as follows:

$$\mathbf{d}_{hi} = \mathbf{d}_h \mathbf{p}_h - \mathbf{d}_i \mathbf{p}_i - \mathbf{b}_h + \mathbf{b}_i$$

$$0 \leq \mathbf{d}_i \leq 1 \text{ and } 0 \leq \mathbf{d}_h \leq 1 \tag{8}$$

\mathbf{d}_h and \mathbf{d}_i are coefficients of two cable lengths. The maximum length of cables is considered, when \mathbf{d}_h and \mathbf{d}_i are in upper value or one. Nonlinear optimization method known as KKT conditions [54, 55] can guarantee the main goal to minimize the norm of \mathbf{d}_{hi} in (8) as a cost function. Several multipliers can solve the optimization problem by equality and inequality constraints. But in this paper, inequality constraints are considered. So, the problem is introduced as follows:

Minimise, $\| \mathbf{d}_{hi} \|_2$
 Subject to:

$$\begin{aligned}
 -\mathbf{d}_h &\leq 0 \\
 \mathbf{d}_h - 1 &\leq 0 \\
 -\mathbf{d}_i &\leq 0 \\
 \mathbf{d}_i - 1 &\leq 0
 \end{aligned} \tag{9}$$

The optimal values of the coefficients \mathbf{d}_h and \mathbf{d}_i can help to find minimum distance. KKT theorem introduces the Lagrange multipliers, λ , with $\lambda_i \geq 0$ and $i = 1, \dots, 4$, as each constraint [46]. The Lagrange function by inequality constraints is introduced as follows:

$$\begin{aligned}
 (\mathbf{d}_h, \mathbf{d}_i, \lambda) &= f(\mathbf{d}_h, \mathbf{d}_i) + \lambda^T \mathbf{h}(\mathbf{d}_h, \mathbf{d}_i) \\
 f(\mathbf{d}_h, \mathbf{d}_i) &= \min \| \mathbf{d}_{hi} \|_2 = \min \| \mathbf{d}_h \mathbf{p}_h - \mathbf{d}_i \mathbf{p}_i - \mathbf{b}_h + \mathbf{b}_i \|_2, \\
 \lambda_T &= [\lambda_1 \ \lambda_2 \ \lambda_3 \ \lambda_4], \\
 \mathbf{h}(\mathbf{d}_h, \mathbf{d}_i) &= \begin{bmatrix} -\mathbf{d}_h \\ \mathbf{d}_h - 1 \\ -\mathbf{d}_i \\ \mathbf{d}_i - 1 \end{bmatrix}
 \end{aligned} \tag{10}$$

Meziane et al. [46] introduced the simplified equation with all conditions and cases. Different \mathbf{d}_h and \mathbf{d}_i can be generated while Lagrange multipliers are activated and deactivated. However, λ_1 and λ_2 or λ_3 and λ_4 could not be activated simultaneously, since \mathbf{d}_h (or \mathbf{d}_i) cannot accept two values. Some cases are not acceptable when \mathbf{d}_i is at the upper limit of the inequality constraint. In this situation, the lengths of cables are in high position; therefore, there is no collision between human and cables. But when \mathbf{d}_i is at the lower limit of the inequality constraint or free, the collision between the human and the cables could be occurring. Six cases are introduced as follows:

Case 1: \mathbf{d}_h and \mathbf{d}_i are found by the inequality constraints. Indeed, $0 \leq \mathbf{d}_h \leq 1$ and $0 \leq \mathbf{d}_i \leq 1$. The Lagrange multipliers are free $\lambda_h = 0$. So, (10) can be observed as follows.

$$\begin{bmatrix} \mathbf{p}_h^T \mathbf{p}_h & -\mathbf{p}_h^T \mathbf{p}_i \\ -\mathbf{p}_i^T \mathbf{p}_h & \mathbf{p}_i^T \mathbf{p}_i \end{bmatrix} \begin{bmatrix} \mathbf{d}_h^* \\ \mathbf{d}_i^* \end{bmatrix} = \begin{bmatrix} \mathbf{p}_h^T \mathbf{b}_{hi} \\ -\mathbf{p}_i^T \mathbf{b}_{hi} \end{bmatrix} \tag{11}$$

while: $\mathbf{b}_{hi} = \mathbf{b}_h - \mathbf{b}_i$

Case 2: \mathbf{d}_i is located at the lower limit of the inequality constraint and \mathbf{d}_h is free. Therefore, $\lambda_3 = 1$ is active, and $\lambda_1 = \lambda_2 = 0$ deactivated as well $\lambda_4 = 0$.

$$\begin{cases} \mathbf{d}_h^* = \frac{p_h^T b_{hi}}{p_h^T p_h} \\ \mathbf{d}_i^* = 0 \end{cases} \tag{12}$$

Case 3: \mathbf{d}_h is the upper limit of the inequality constraint and \mathbf{d}_i is free. So, $\lambda_2 = 1$ is active and $\lambda_3 = \lambda_4 = 0$ deactivated.

$$\begin{cases} \mathbf{d}_h^* = 1 \\ \mathbf{d}_i^* = \frac{p_i^T p_h - p_i^T b_{hi}}{p_i^T p_i} \end{cases} \tag{13}$$

Case 4: when \mathbf{d}_h is located at the lower limit of the inequality constraint and \mathbf{d}_i is free, so $\lambda_1 = 1$ is active and $\lambda_3 = \lambda_4 = \lambda_2 = 0$ is deactivated.

$$\begin{cases} \mathbf{d}_h^* = 0 \\ \mathbf{d}_i^* = \frac{-p_i^T b_{hi}}{p_i^T p_i} \end{cases} \tag{14}$$

Case 5: \mathbf{d}_h is at the upper limit of the inequality constraint and \mathbf{d}_i is at the lower limit. Indeed $\lambda_1 = 1, \lambda_4 = 1$ are active, and $\lambda_2 = \lambda_3 = 0$ is deactivated.

$$\begin{cases} \mathbf{d}_h^* = 1 \\ \mathbf{d}_i^* = 0 \end{cases} \tag{15}$$

Case 6: \mathbf{d}_h and \mathbf{d}_i are located at the lower limit of the constraints. $\lambda_1 = \lambda_3 = 1$ is activated and $\lambda_2 = \lambda_4 = 0$ is deactivated.

$$\begin{cases} \mathbf{d}_h^* = 0 \\ \mathbf{d}_i^* = 0 \end{cases} \tag{16}$$

Cable–human collision can be considered as two-line interference. A collision is detected when two lines get close to each other to a certain threshold value.

The next step is computation of \mathbf{d}_{hi} for each value \mathbf{d}_h and \mathbf{d}_i . The distance \mathbf{d}_{hi} are the distance between the two points \mathbf{B}_h and \mathbf{B}_i . The algorithm for the computation of the shortest distance between human and cables can be seen in Fig. 5. The first cable is selected, then coefficients for all six cases can be determined. In this case where the constraints are satisfied, the shortest distance according to (8) is then estimated. Hence, the computed shortest distance is compared with a threshold value such that the shortest distance value is increased by relocating vertically up and down the corresponding attachment point until the shortest distance between cables and human exceeds the threshold value, which means that the collision has been avoided, as it is discussed in later sections. The relocation theory of attachment points is discussed in the next section.

3.6. Cable interference avoidance – relocation of corresponding attachment points

After solving the inverse kinematics and the computation of the shortest distance between human and cables, the attachment points on the rails are relocating to solve the collision between cables and human while maintaining the end effector trajectory.

The shortest distance computation between human and cables depends on position of the human arm and the cables that can be found according to position of the attachment points on reels and the attachment points on end effector. In case of a near collision between human and cable i ($i = 1$ to 8), the reel moves up or down when \mathbf{d}_{hi} is lower than threshold. Therefore, the position of the reel i on the rail is displaced by a step as scalar Δq . Parameter Δq is fixed at 1.5% of the distance between two attachment points on the one rail in Z direction. In this research, parameter Δq is selected theoretically 0.1 m. So, the new location of the attachment point $(\tilde{\mathbf{q}}_{iz})_{k+1}$ or $(\tilde{\mathbf{q}}_{iz})_{new}$ is updated as follows: where the previous location of the attachment point $(\tilde{\mathbf{q}}_{iz})_{initial}$ or $(\tilde{\mathbf{q}}_{iz})_k$ moves as Δq on the rail:

$$(\tilde{\mathbf{q}}_{iz})_{k+1} = (\tilde{\mathbf{q}}_{iz})_k + \Delta q, (\tilde{\mathbf{q}}_{iz})_k = (z_i)_k \tag{17}$$

k : actual sampling time
 $k + 1$: next sampling time

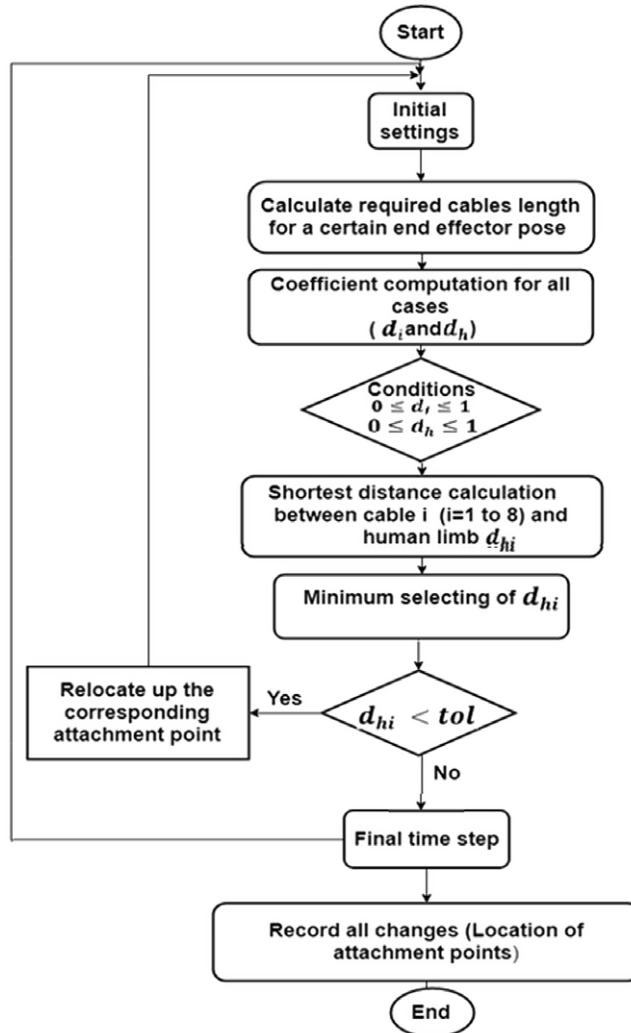


Figure 5. Collision avoidance algorithm.

z_i : position of attachment points in Z direction on the rail

$$\Delta q = \begin{cases} 0 & \text{if there is not collision between human and cables} \\ 0.1 & \text{if there is collision between human and cables} \end{cases}$$

This theory can be valid by constraining the maximum vertical location of a reel on the rail where the attachment point should not overpass. The location of the reel can move vertically by a servo linear actuator. This idea of reconfiguration to avoid collision between cables and human limb simulated in Matlab is presented in Section 4.

4. Simulation of shortest distance cable–human collision avoidance

Relocation of the attachment points on the rails to avoid a collision between cables and humans is this project’s main goal. Matlab script is used to detect and eliminate cable–human interference in simulation.

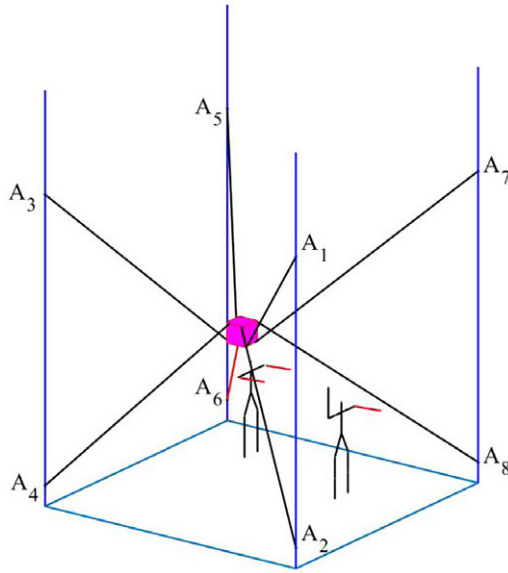


Figure 6. *Two humans in shared workspace.*

In Sections 4.1, three positions (close to cables 8, 6, and 2) are selected to perform the presented algorithm when human is placed in different parts of the workspace. The algorithm avoids collision between human limbs and cables while the end effector keeps the trajectory unchanged, as shown in supplementary material, Video 1: (Experiment 1: One human in the workspace) [56]. A simple inverse kinematics approach is used regarding the predefined trajectory and position of attachment points. Section 4.2 presents the feasible wrench workspace when a human is located near cables 8, 6, and 2, as shown in supplementary material, Video 1: (Experiment 1: One human in the workspace) [56]. To show the ability of the algorithm to avoid collision between humans and cables, two or more humans are added to the workspace in Section 4.3, as shown in supplementary material, Video 2: Experiment 2 (Two humans in the workspace) [57]. The 3D view of the one human is shown in Fig. 1. Two humans in the shared workspace are indicated in 3D, as shown in Fig. 6.

The method presented in this paper can be applied to three-dimensional objects. Whereas each 3D geometry can be represented by triangle mesh which comprises a set of triangles (connected by their edges), the 3D model of whole human body or other obstacles can be used for this suggested method.

Regarding the trajectory computation point, simple inverse kinematics approach is used, where the trajectory is defined previously. The number of AFLO (Algorithm Floating-point Operation) of the code in Matlab is estimated at 278 for four functions inside the algorithm presented in Fig. 5. This algorithm is presented as follows (for each iteration):

1. Shortest distance computation between human and each cable with 147 AFLO
2. Collision avoidance algorithm with 11 AFLO
3. Cable length computation for each iteration with 24 AFLO
4. Cable tension computation for each iteration with 96 AFLO

An iteration corresponds to an update of the setpoint of the tensile force and pose which are submitted to the robot closed-loop controller. Meanwhile, capacity in GFLOPS of the computer [58] is 161, while the sampling period is 1 msec. The total execution time of the suggested algorithm is estimated at $1.72670807e-9$ which is less than 70% sampling time $1.72670807e-9 < 0.007$. The execution time is

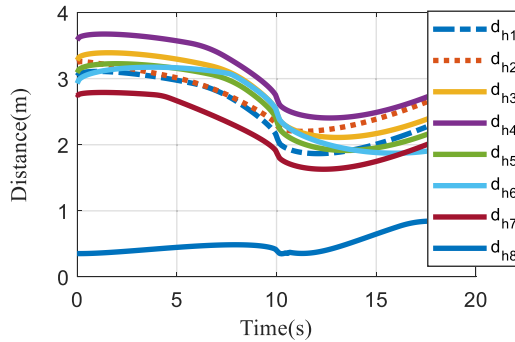


Figure 7. Shortest distance between cables and human near cable 8 (circular trajectory).

evaluated using this equation:

$$\text{Execution time} = \frac{\text{AFLO (Algorithm Floating point Operation) in the algorithm}}{\text{Capacity in FLOPS of the computer}} \quad (18)$$

The capacity of the computer is evaluated using Linepack Xtreme x64 for Windows which estimates the number of FLOPS. The number of floating-point operations of the suggested algorithm (AFLO) is estimated using ref. [59]. In hard real-time application, the overall algorithm has to be less than 70% of the sampling period. Although, there is currently no physical model of the robot, it is possible to state that the suggested algorithm can operate in real time in the presence of a physical model of a cable-driven parallel robot.

Section 4.1 discusses the results of collision avoidance between one human and two humans with cables in shared workspace.

4.1 Results

The presented method can determine the shortest distance as collision detection. If the shortest distance is lower than tolerance and close to collision, the algorithm moves the attachment point on rails and updates the cable lengths. The results of the shortest distance between cables and human can be seen in Fig. 7 for three situations when human is close to cables 8, cable 2, and cable 6 for circular trajectory. The end effector tracks the circular trajectory (as the desired trajectory) presented by Youssef and Otis [29]. To guarantee human safety, the threshold between human and cable is considered as 0.35 m.

As shown in Fig. 7 when human is near cable 8, all cables except cable 8 are at acceptable distance from human limb. The distance between human near cable 8 and cables are d_{hi} . It can be observed that the distance between cable 8 and human is less than threshold, and the position of cable 8 needs to be modified to avoid cable–human collision. Therefore, Fig. 8 shows that there is no change in the position of reels 1 to 7. The reels 2,4, and 6 are located at 0.5 m, and the reels 1, 3, 5, and 7 are located at 7.5 m.

Figure 9 demonstrates the shortest distance between cable 8 and human and the relocation of attachment point 8. When the shortest distance between human and cable 8 falls below the threshold, detected by an algorithm at around 10 s, the relocation of attachment points on reels could avoid collision between cable 8 and the human limb. So, the distance is increased until the distance between cable 8 and human reaches a reliable distance and above the threshold.

To investigate the performance of the proposed method, the results have been obtained when human is close to cable 2 and cable 6. Figure 10(b-1) shows the distance between human and cable 2 when human is located close to cable 2 and Figure 10(a-1) indicates the distance between human and cable 6 when human is placed near cable 6. There are four points that distance between human and cable 6 is in threshold, and three threshold points in distance between human and cable 2 can be seen in Fig. 10(b-2).

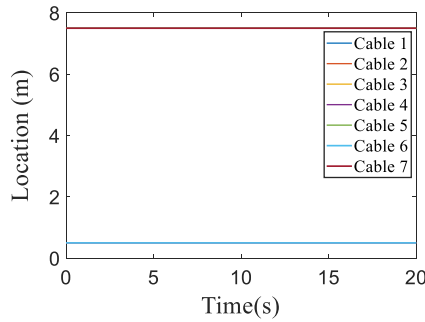


Figure 8. Attachment point location of cables 1 to 7 – human near cable 8.

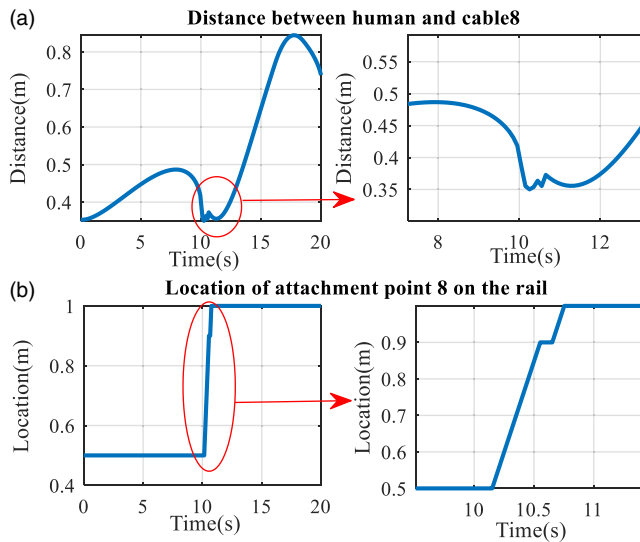


Figure 9. Circular trajectory: (a) shortest distance between cable 8 and human (human is placed near cable 8) and (b) attachment point location of cable 8.

Figure 11 indicates the length of cables for all three situations. According to Fig. 11, there are changes suddenly in length of cables because of close distance between cable 8 and skeleton placed near cable 8 in Fig. 11(a), between human and cable 6 in Fig. 11(b) when human model is located near cable 6 and between human and cable 2 in Fig. 11(c).

4.2 The wrench feasible workspace

Firstly, cables tension distribution equation can be solved to map feasible workspace. The computational algorithm is used to map the reconfigurable workspace. Figure 12 indicates the initial (blue) and final (red) workspaces according to the reconfiguration of the mechanism due to circular motion of end effector and distance between human arm and cable 2, 6, and 8.

As it can be observed in Fig. 12, final workspace is changed due to relocation of the attachment points on the rail, while trajectory of the end effector kept unchanged. Upper attachment points (1, 3, 5, and 7) are located Initially at 7.5 m. In Fig. 13, cable 8 was initially at 0.5 m and is moving to 1 m to avoid collision when human is located near cable 8. As can be seen in Fig. 12(a), the top part of the final workspace and the initial workspace are same. This can be clearly observed by comparing between the X–Z views Fig. 12(b). Meanwhile, there was no noteworthy change by comparing initial and final

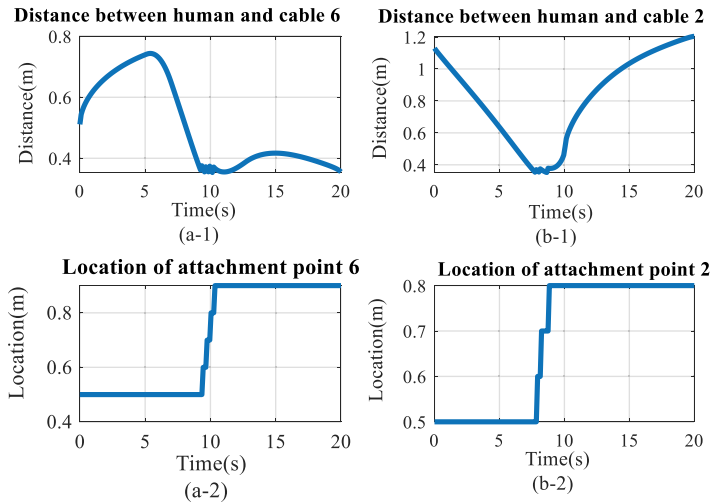


Figure 10. Circular trajectory: (a-1) distance between human and cable 6 (human is located close to cable 6), (a-2) attachment point position of cable 6 on the rail, (b-1) distance between human and cable 2 (human is located close to cable 2), and (b-2) attachment point position of cable 2 on the rail.

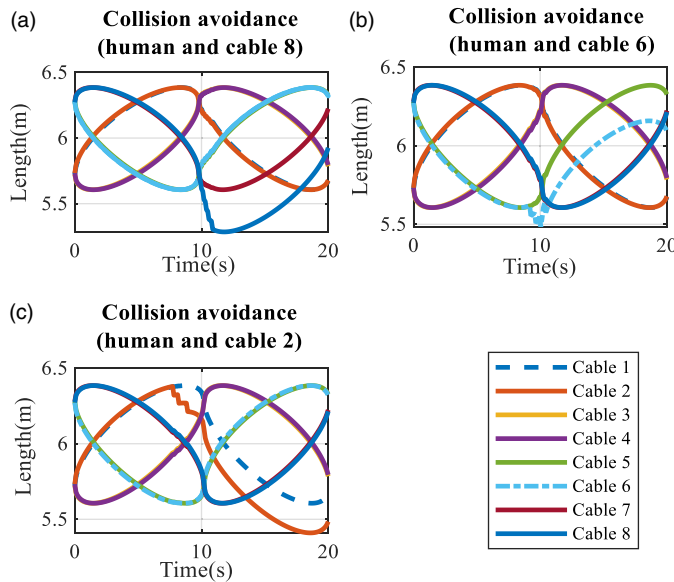


Figure 11. Length of cables (circular trajectory): (a) human near cable 8, (b) human near cable 6, and (c) human near cable 2.

workspace the X–Y views (Fig. 12(d)) or the Y–Z views Fig. (12 c). The results for two other situations are observed in Figs. 13 and 14. The attachment point 2 in Fig. 13(b) is moved from 0.5 to 0.8 m. This movement could prove Fig. 12 where five points in threshold distance is observed. Also, Fig. 14(c) indicates initial and final workspaces when human is near cable 6; meanwhile, the attachment point 6 can be moved from 0.5 to 0.9 m in order to avoid collision between human and cable 6.

Figures 15, 16, and 17 indicate the difference between original and final workspaces and are presented by the boundary of some points of the end effector’s position in an original workspace that cannot be

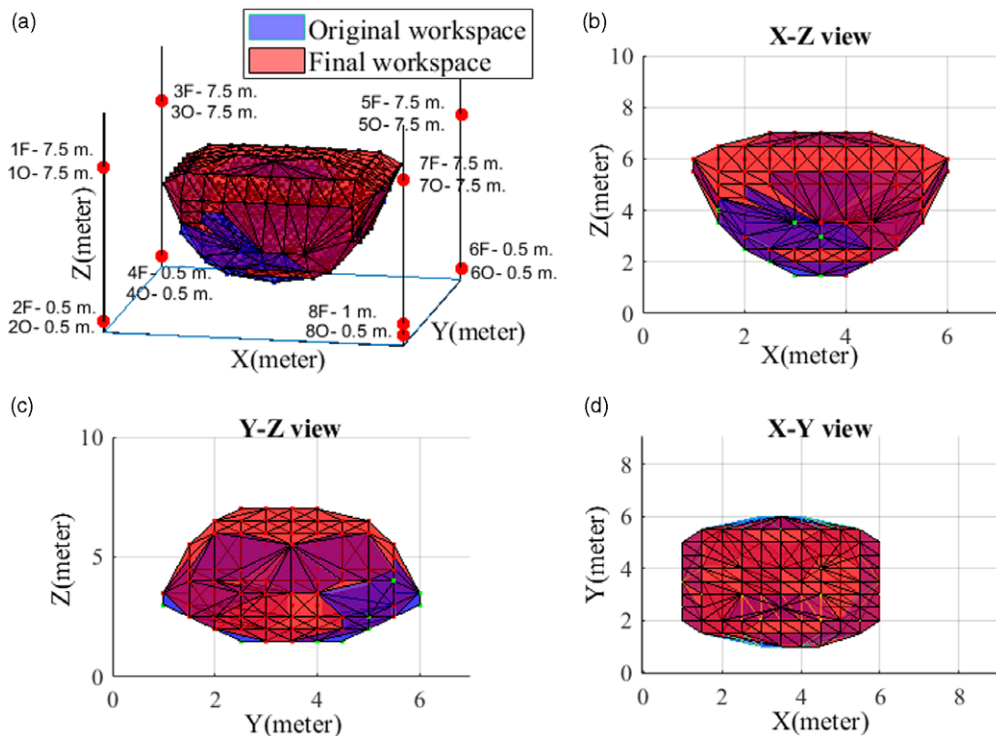


Figure 12. Circular trajectory (cables–human collision when human is near cable 8): (a) final and original workspaces 3D, (b) front view, (c) side view, and (d) top view.

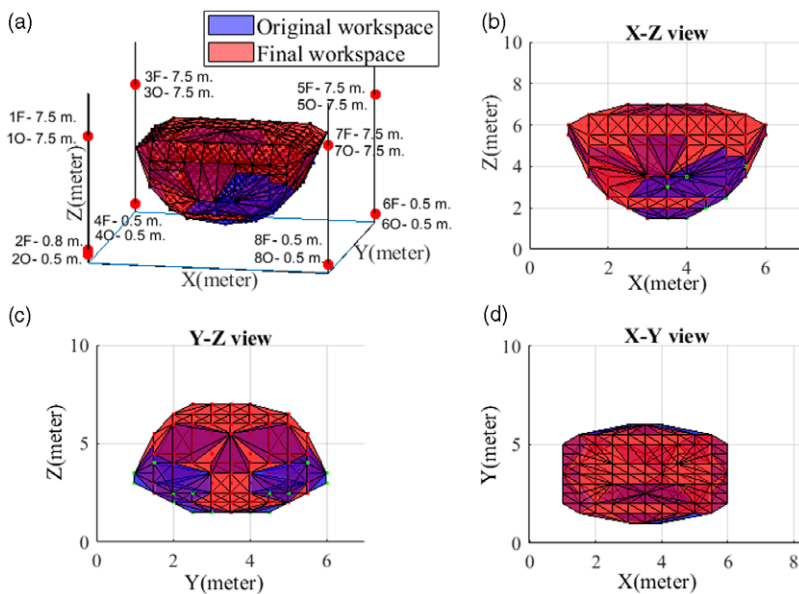


Figure 13. Circular trajectory (cables–human collision when human is near cable 2): (a) final and original workspaces 3D, (b) front view, (c) side view, and (d) top view.

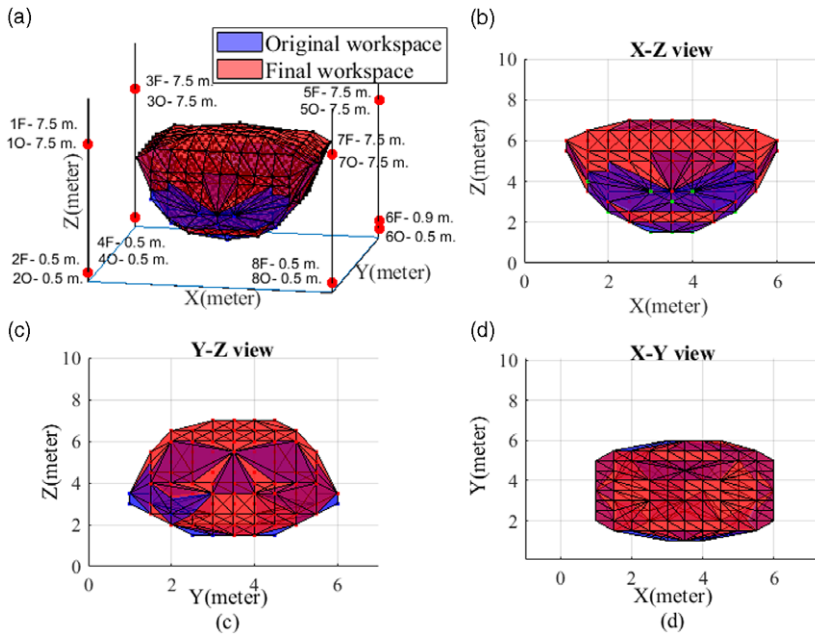


Figure 14. Circular trajectory (cables–human collision when human is near cable 6): (a) final and original workspaces 3D, (b) front view, (c) side view, and (d) top view.

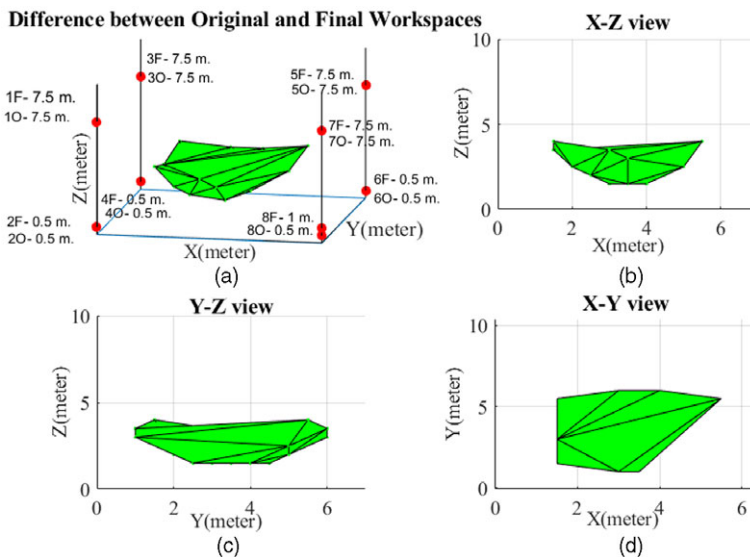


Figure 15. Difference between original and final workspaces when human is near cable 8: (a) difference between final and original workspace 3D, (b) front view, (c) side view, and (d) top view.

found in the final workspace. As can be seen in Figs. 15, 16, and 17, the final workspace is strictly smaller at the bottom part due to a change in the position of the attachment points on rails 8, 6, and 2. The position of the upper attachment points does not change in the initial and final workspace, and the final trajectory is inside the initial workspace.

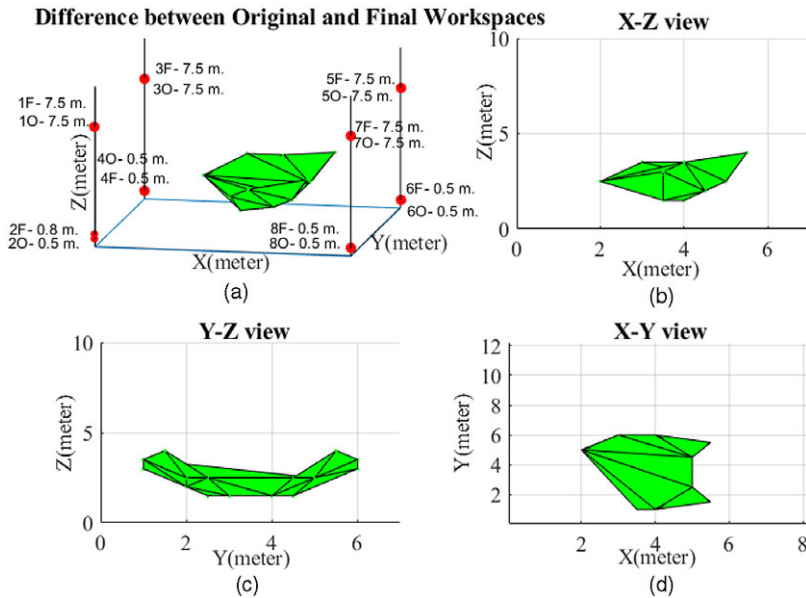


Figure 16. Difference between original and final workspaces when human is near cable 2: (a) difference between final and original workspace 3D, (b) front view, (c) side view, and (d) top view.

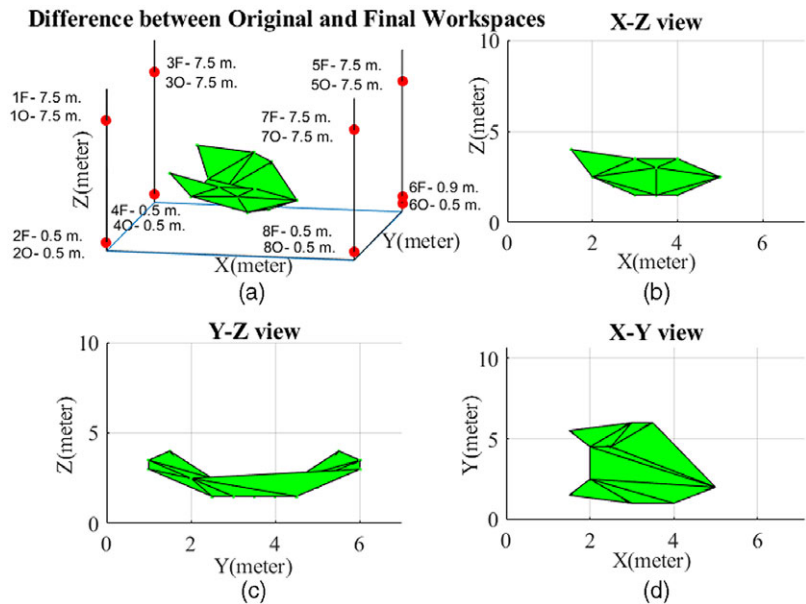


Figure 17. Difference between original and final workspaces when human is near cable 6: (a) difference between final and original workspace 3D, (b) front view, (c) side view, and (d) top view.

4.3 Two humans inside the workspace

The risk of collision between humans and robots could be raised when many humans are in the workspace. The suggested algorithm can avoid collision between all humans and each cable. In addition of collision avoidance between one human and cables, collision avoidance between two humans located in the hybrid workspace generating up to three collision avoidances simultaneously using reel position

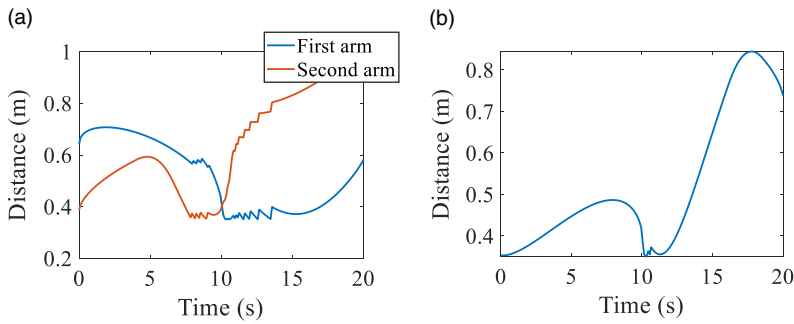


Figure 18 (a) Distance between both first human arms and cable 6 and (b) distance between second human arm and cable 8.

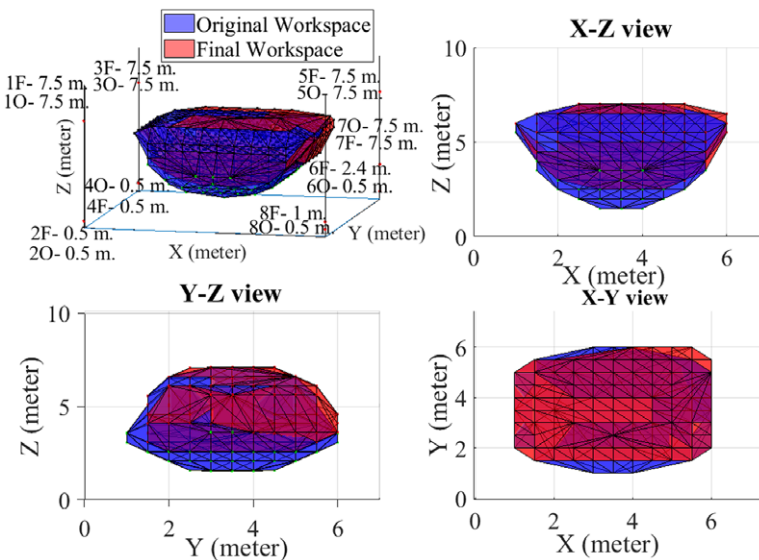


Figure 19. Original and final workspaces.

relocalization strategy is discussed in this section. At the same time, the endeffector keeps its original trajectory setpoint. These two humans are in the workspace near cables 6 and 8. In this section, the first human #1 is located near cable 6 while both arms are moving, and the second one is located near cable 8 while only one arm of this human is moving. Figure 18 demonstrates the collision avoidance between the first arm of human #1 with cable 6 for 11 times. This algorithm avoids collision between left arm of human with cable 6 for 8 times.

Finally, as shown in Fig. 19, the algorithm moves attachment point 6 from 0.5 to 2.4 m. Meanwhile, moving attachment point 8 from 0.5 m to 1 m is indicated in Fig. 19 to avoid collision between the second human and cable 8. The first human moves both arms while one of the second human arms moves simultaneously through the workspace. Supplementary material, Video 2: Experiment 2 (Two humans in the workspace-Part 2) [57] shows that attachment point 8 moves up (from 0.5 to 0.9 m) when the first human is located near cable 8. Meanwhile, the attachment point 6 moves up 1.9 m (from 0.5 to 2.4 m), while the end effector keeps its trajectory in the WCW.

5. Limitation of the study

Applications for cable-driven parallel robot have very high marketing potential as long as safety solutions are validated, which are highly complex on academic prototypes with a low level of maturity. So, the focus on large, shared workspace, while human safety is guaranteed, is the main contribution of this paper, but of course highly difficult to evaluate on a real installation.

The first limitation of this study is the experimentation using a full-scale CDPM. For safety issue, this paper does not present real-case experiment since the prototype do not have CSA Z434-14, 16, 18, 19 (ISO 10281) certifications (among others such as electric enclosure and control certification). The CDPM's large workspaces could allow high velocity of the mobile part and could be highly dangerous for any participants. One risk comes from potential software bugs and broken hardware (motor encoders malfunction, etc.). A technical solution is proposed in this paper to ensure the safety of the human operator working in collaboration with the CDPR, but bugs and broken hardware are still not managed. Moreover, with a true, scaled installation, another challenge will be ethical issue for doing experimentation with human participants. As the CSA/ISO certification is not achieved, it is not possible to get an ethical certificate from Research Ethics Board (REB) Committee.

A second limitation of this paper is cable and reel modeling, considering the model of cables could make the system more realistic for the position/velocity control in the simulation. As suggested in refs. [18, 19], in this paper, the cables are assumed massless, and straight-line segments without sagging due to small size of suggested CDPM and the attachment points are simplified to ideal points [21] like many papers such as refs. [60–62].

Meanwhile, as third limitation, the inertia is not considered since the inertia of the cables is negligible compared to inertia of the end effector combined with the payload while using spectra cable in the size and dimension of our current CDPM. To ignore the cable inertia effect, the suggested method assumes also that the motion of the end effector is slow (Tool Center Point limited to 250 mm/sec and 150 N, during operation processes in order to meet ISO 10281), and a rate limiter is used in the algorithm (under the prescribed standard for human–robot collaboration in the same workspace) Safety of Robot Integration [63]). Although high velocities and accelerations can be generated in CDPM (low inertia of end effector, cables, and reels), it is forbidden in human–robot interaction according to CSA Z434 (ISO 10281).

In such limitations, cable vibration, cable sagging, reel, and models (such as static and dynamic models) are negligible in the simulation results presented in this paper. As velocity is limited for human–robot direct interaction, vibration is limited and could come from friction in a real-scale CDPM. These hypothesis (which are much more facts) are taken in this paper.

Finally, another limitation is data extraction from sensors. The data of human limb positions are collected from sensors, so there are some limitations due to sensors, such as Kinect, which provide lines to model limbs. Moreover, these limitations must be considered in order to guarantee the human safety by keeping a minimal distance between each cable and all segments representing the human limbs.

6. Conclusion and future works

CDPM industrial applications should be chosen with very high potential to market as long as safety solutions are validated, which is highly complex on the academic prototype with a low level of maturity. So, the focus on large, shared workspace CDPM, while human safety is guaranteed, is the main contribution of this paper. This paper demonstrates that CDPMs can be used for collaborative tasks with humans in the same workspace and proposes a technical solution to ensure the safety of the human operator.

In this study, a new model of a reconfigurable, fully constrained cable-driven parallel robot based on the relocation of the attachment points on the rail is presented. In this reconfiguration model, the attachment points on the rails can be movable, unlike conventional CDPM, where attachment points on the bases are fixed. The idea is collision avoidance between humans and cables while maintaining the desired trajectory of the end effector unchanged, which is limited by the mechanism's kinetostatic

capabilities. A proposed algorithm can detect collision between cables and human limbs using the KKT method and moves up and down the attachment points vertically on the given rail to increase the shortest distance between humans and cables to the safe threshold. This new approach was simulated by circular trajectories. So, the algorithm effectively detected a near collision between cables 2, 6, and 8 with the human limb during a circular trajectory of the end effector and increased attachment points' location to a safe position. Finally, as can be seen in the results, the workspace is valid when the attachment points on reels are moved.

In future works, a robust controller can be designed to update the pose of the end effector, while the reconfiguration theory is used to avoid collision between cables and humans. A new algorithm to compute boundary workspace can be suggested. Reconfiguration theory by changing attachment points on the end effector can be evaluated for fully constrained CDPM. Meanwhile, the artificial potential field method can be extended in reconfiguration CDPM to estimate the safe relocation of attachment points on the rails.

Supplementary material. To view supplementary material for this article, please visit <https://doi.org/10.1017/S0263574722000996>

Funding. This work received financial support from the Fonds de recherche du Québec – Nature et technologies (FRQNT), under grant number 2020-CO-275043 and grant number 2016-PR-188869. This project uses the infrastructure obtained by the Ministère de l'Économie et de l'Innovation (MEI) du Québec, John R. Evans Leaders Fund of the Canadian Foundation for Innovation (CFI), and the Infrastructure Operating Fund (FEI) under the project number 35395. Other financial support was used in this project. Natural Sciences and Engineering Research Council of Canada (NSERC) Discovery Grant number RGPIN-2018-06329.

References

- [1] X. Xu, Y. Lu, B. Vogel-Heuser and L. Wang, "Industry 4.0 and Industry 5.0—Inception, conception and perception," *J. Manuf. Syst.* **61**(April 2), 530–535 (2021).
- [2] K. A. Demir, G. Döven and B. Sezen, "Industry 5.0 and human-robot co-working," *Proc. Comput. Sci.* **158**(2), 688–695 (2019).
- [3] R. Meziane, M. J.-D. Otis and H. Ezzaidi, "Human-robot collaboration while sharing production activities in dynamic environment: SPADER system," *Robot. Comput.-Integr. Manuf.* **48**(2), 243–253 (2017).
- [4] J. Albus, R. Bostelman and N. Dagalakis, "The NIST SPIDER, a robot crane," *J. Res. Natl. Inst. Stan.* **97**(3), 373 (1992).
- [5] M. J.-D. Otis, T. L. Nguyen-Dang, T. Laliberte, D. Ouellet, D. Laurendeau and C. Gosselin, "Cable tension control and analysis of reel transparency for 6-dof haptic foot platform on a cable-driven locomotion interface," *Int. J. Electr. Electron. Eng.* **3**(1), 16–29 (2009).
- [6] S. Kawamura, H. Kino and C. Won, "High-speed manipulation by using parallel wire-driven robots," *Robotica* **18**(1), 13–21 (2000).
- [7] N. Zhang, W. Shang and S. Cong, "Dynamic trajectory planning for a spatial 3-DoF cable-suspended parallel robot," *Mech. Mach. Theory* **122**(1), 177–196 (2018).
- [8] M. A. Khosravi and H. D. Taghirad, "Robust PID control of fully-constrained cable driven parallel robots," *Mechatronics* **24**(2), 87–97 (2014).
- [9] M. Gouttefarde, "Characterizations of Fully Constrained Poses of Parallel Cable-Driven Robots: A Review," **In: International Design Engineering Technical Conferences and Computers and Information in Engineering Conference** (2008).
- [10] P. Bosscher, A. T. Riechel and I. Ebert-Uphoff, "Wrench-feasible workspace generation for cable-driven robots," *IEEE Trans. Robot.* **22**(5), 890–902 (2006).
- [11] W. B. Lim, G. Yang, S. H. Yeo and S. K. Mustafa, "A generic force-closure analysis algorithm for cable-driven parallel manipulators," *Mech. Mach. Theory* **46**(9), 1265–1275 (2011).
- [12] C. B. Pham, S. H. Yeo, G. Yang, M. S. Kurbanhusen and I. M. Chen, "Force-closure workspace analysis of cable-driven parallel mechanisms," *Mech. Mach. Theory* **41**(1), 53–69 (2006).
- [13] E. Ottaviano and G. Castelli, "A Study on the Effects of Cable Mass and Elasticity in Cable-Based Parallel Manipulators," **In: ROMANSY 18 Robot Design, Dynamics and Control**, (Springer, 2010) pp. 149–156.
- [14] K. Kozak, Q. Zhou and J. Wang, "Static analysis of cable-driven manipulators with non-negligible cable mass," *IEEE Trans. Robot.* **22**(3), 425–433 (2006).
- [15] N. Riehl, M. Gouttefarde, S. Krut, C. Baradat and F. Pierrot, "Effects of Non-Negligible Cable Mass on the Static Behavior of Large Workspace Cable-Driven Parallel Mechanisms," **In: IEEE International Conference on Robotics and Automation** (IEEE, 2009).
- [16] E. Ottaviano, A. Arena and V. Gattulli, "Geometrically exact three-dimensional modeling of cable-driven parallel manipulators for end-effector positioning," *Mech. Mach. Theory* **155**, 104102 (2021).

- [17] X. Weber, L. Cuvillon and J. Gangloff, "Active Vibration Canceling of A Cable-Driven Parallel Robot in Modal Space," **In: IEEE International Conference on Robotics and Automation (ICRA)** (IEEE, 2015).
- [18] A. Ming, "Study on multiple degree-of-freedom positioning mechanism using wires (part 2)-development of a planar completely restrained positioning mechanism," *Int. J. JSPE* **28**(3), 235 (1994).
- [19] R. G. Roberts, T. Graham and T. Lippitt, "On the inverse kinematics, statics, and fault tolerance of cable-suspended robots," *J. Robot. Syst.* **15**(10), 581–597 (1998).
- [20] A. Pott, "Influence of Pulley Kinematics on Cable-Driven Parallel Robots," **In: Latest Advances in Robot Kinematics** (Springer, 2012) pp. 197–204.
- [21] P. Miermeister and A. Pott, "Modelling and Real-Time Dynamic Simulation of the Cable-Driven Parallel Robot IPAnema," **In: New Trends in Mechanism Science** (Springer, 2010) pp. 353–360.
- [22] D. Q. Nguyen and M. Gouttefarde, "On the Improvement of Cable Collision Detection Algorithms," **In: Cable-Driven Parallel Robots** (Springer, 2015) pp. 29–40.
- [23] T. Makino and T. Harada, "Cable Collision Avoidance of A Pulley Embedded Cable-Driven Parallel Robot By Kinematic Redundancy," **In: Proceedings of the 4th International Conference on Control, Mechatronics and Automation** (2016).
- [24] S. Lahouar, E. Ottaviano, S. Zeghoul, L. Romdhane and M. Ceccarelli, "Collision free path-planning for cable-driven parallel robots," *Robot. Auton. Syst.* **57**(11), 1083–1093 (2009).
- [25] L. Gagliardini, M. Gouttefarde and S. Caro, "Design of Reconfigurable Cable-Driven Parallel Robots," **In: Mechatronics for Cultural Heritage and Civil Engineering** (Springer, 2018) pp. 85–113.
- [26] F. Trautwein, T. Reichenbach, A. Pott and A. Verl, "Workspace Planning for In-Operation-Reconfiguration of Cable-Driven Parallel Robots," **In: International Conference on Cable-Driven Parallel Robots** (Springer, 2021).
- [27] J. Xu and K.-S. Park, "Moving obstacle avoidance for cable-driven parallel robots using improved RRT," *Microsyst. Technol.* **27**(6), 2281–2292 (2021).
- [28] M. FarzanehKaloorazi, M. T. Masouleh and S. Caro, "Collision-free workspace of parallel mechanisms based on an interval analysis approach," *Robotica* **35**(8), 1747–1760 (2017).
- [29] K. Youssef and M. J.-D. Otis, "Reconfigurable fully constrained cable driven parallel mechanism for avoiding interference between cables," *Mech. Mach. Theory* **148**, 103781 (2020).
- [30] J.-P. Merlet and D. Daney, "Legs Interference Checking of Parallel Robots Over A Given Workspace or Trajectory," **In: Proceedings 2006 IEEE International Conference on Robotics and Automation, ICRA 2006** (IEEE, 2006).
- [31] W. Kowalczyk, M. Michałek and K. Kozłowski, "Trajectory tracking control and obstacle avoidance for a differentially driven mobile robot," *IFAC Proc.* Vol. **44**(1), 1058–1063 (2011).
- [32] S. S. Ge and Y. J. Cui, "Dynamic motion planning for mobile robots using potential field method," *Auton. Robot.* **13**(3), 207–222 (2002).
- [33] N. Malone, H. T. Chiang, K. Lesser, M. Oishi and L. Tapia, "Hybrid dynamic moving obstacle avoidance using a stochastic reachable set-based potential field," *IEEE Trans. Robot.* **33**(5), 1124–1138 (2017).
- [34] M. Otte and E. Frazzoli, "RRTX: asymptotically optimal single-query sampling-based motion planning with quick replanning," *Int. J. Robot. Res.* **35**(7), 797–822 (2016).
- [35] X. Yang, L. M. Alvarez and T. Bruggemann, "A 3D collision avoidance strategy for UAVs in a non-cooperative environment," *J. Intell. Robot. Syst.* **70**(1-4), 315–327 (2013).
- [36] A. Chakravarthy and D. Ghose, "Generalization of the collision cone approach for motion safety in 3-D environments," *Auton. Robot.* **32**(3), 243–266 (2012).
- [37] J.-H. Bak, S. W. Hwang, J. Yoon, J. H. Park and J. O. Park, "Collision-free path planning of cable-driven parallel robots in cluttered environments," *Intel. Serv. Robot.* **12**(3), 243–253 (2019).
- [38] B. Zhang, W. Shang and S. Cong, "Optimal RRT* Planning and Synchronous Control of Cable-Driven Parallel Robots," **In: 3rd International Conference on Advanced Robotics and Mechatronics (ICARM)** (IEEE, 2018).
- [39] R. Bordalba, J. M. Porta and L. Ros, "Randomized Kinodynamic Planning for Cable-Suspended Parallel Robots," **In: Cable-Driven Parallel Robots** (Springer, 2018) pp. 195–206.
- [40] Y. Wischnitzer, N. Shvalb and M. Shoham, "Wire-driven parallel robot: permitting collisions between wires," *Int. J. Robot. Res.* **27**(9), 1007–1026 (2008).
- [41] M. M. Aref and H. D. Taghirad, "Geometrical Workspace Analysis of A Cable-Driven Redundant Parallel Manipulator: KNTU CDRPM," **In: IEEE/RSJ International Conference on Intelligent Robots and Systems** (IEEE, 2008).
- [42] A. M. Pinto, E. Moreira, J. Lima, J. P. Sousa and P. Costa, "A cable-driven robot for architectural constructions: a visual-guided approach for motion control and path-planning," *Auton. Robot.* **41**(7), 1487–1499 (2017).
- [43] B. Wang, B. Zi, S. Qian and D. Zhang, "Collision Free Force Closure Workspace Determination of Reconfigurable Planar Cable Driven Parallel Robot," **In: Asia-Pacific Conference on Intelligent Robot Systems (ACIRS)** (IEEE, 2016).
- [44] L. Blanchet and J.-P. Merlet, "Interference Detection for Cable-Driven Parallel Robots (CDPRs)," **In: 2014 IEEE/ASME International Conference on Advanced Intelligent Mechatronics** (IEEE, 2014).
- [45] M. J.-D. Otis, S. Perreault, T. L. Nguyen-Dang, P. Lambert, M. Gouttefarde, D. Laurendeau and C. Gosselin, "Determination and management of cable interference between two 6-DOF foot platforms in a cable-driven locomotion interface," *IEEE Trans. Syst. Man Cybern. A Syst. Hum.* **39**(3), 528–544 (2009).
- [46] R. Meziane, P. Cardou and M. J.-D. Otis, "Cable interference control in physical interaction for cable-driven parallel mechanisms," *Mech. Mach. Theory* **132**(03), 30–47 (2019).
- [47] M. Rushton and A. Khajepour, "Planar variable structure cable-driven parallel robots for circumventing obstacles," *J. Mech. Robot.* **13**(2), 021011 (2021).

- [48] M. Anson, A. Alamdari and V. Krovi, "Orientation workspace and stiffness optimization of cable-driven parallel manipulators with base mobility," *J. Mech. Robot.* **9**(3), 709 (2017).
- [49] L. Barbazza, F. Oscari, S. Minto and G. Rosati, "Trajectory planning of a suspended cable driven parallel robot with reconfigurable end effector," *Robot. Comput.-Integr. Manuf.* **48**(1), 1–11 (2017).
- [50] S. Haddadin, A. Albu-Schäffer and G. Hirzinger, "Requirements for safe robots: measurements, analysis and new insights," *Int. J. Robot. Res.* **28**(11-12), 1507–1527 (2009).
- [51] Q. Duan and X. Duan, "Workspace classification and quantification calculations of cable-driven parallel robots," *Adv. Mech. Eng.* **6**(2), 358727 (2014).
- [52] J. J. Moré, "The Levenberg-Marquardt Algorithm: Implementation and Theory," *In: Numerical Analysis* (Springer, 1978) pp. 105–116.
- [53] M. J.-D. Otis, T. L. Nguyen-Dang, D. Laurendeau and C. Gosselin, "Interference Estimated Time of Arrival on A 6-DOF Cable-Driven Haptic Foot Platform," *In: IEEE International Conference on Robotics and Automation* (IEEE, 2009).
- [54] H. D. Taghirad and Y. B. Bedoustani, "An analytic-iterative redundancy resolution scheme for cable-driven redundant parallel manipulators," *IEEE Trans. Robot.* **27**(6), 1137–1143 (2011).
- [55] M. Carricato and J.-P. Merlet, "Geometrico-static Analysis of Under-Constrained Cable-Driven Parallel Robots," *In: Advances in Robot Kinematics: Motion in Man and Machine* (Springer, 2010) pp. 309–319.
- [56] E. Khoshbin, K. Youssef, R. Meziane and M. J.-D Otis, Reconfigurable fully constrained cable driven parallel mechanism for avoiding collision between cables with human, supplementary material, Video 1, Experiment 1: One human in the workspace (May 2022).
- [57] E. Khoshbin, K. Youssef, R. Meziane and M. J.-D Otis, Reconfigurable fully constrained cable driven parallel mechanism for avoiding collision between cables with human, supplementary material, Video 2, Experiment 2: Two humans in the workspace (May 2022).
- [58] J. Issa, "Performance and power analysis for high performance computation benchmarks," *Central Eur. J. Comput. Sci.* **3**(1), 1–16 (2013).
- [59] H. Qian, *Counting the floating point operations (FLOPS)* (<https://www.mathworks.com/matlabcentral/fileexchange/50608-counting-the-floating-point-operations-flops>), MATLAB central file exchange. Retrieved May 8, 2022.
- [60] K. M. Youssef, *Reconfigurable cable driven parallel mechanism* (Université du Québec à Chicoutimi, 2020).
- [61] Z. Zake, F. Chaumette, N. Pedemonte and S. Caro, "Vision-based control and stability analysis of a cable-driven parallel robot," *IEEE Robot. Automat. Lett.* **4**(2), 1029–1036 (2019).
- [62] W. Kraus, V. Schmidt, P. Rajendra and A. Pott, "System Identification and Cable Force Control for A Cable-Driven Parallel Robot with Industrial Servo Drives," *In: 2014 IEEE International Conference on Robotics and Automation (ICRA)* (IEEE, 2014).
- [63] ISO 10218-2: 2011: *Robots and Robotic devices-Safety Requirements for Industrial Robots-Part 2: Robot Systems and Integration* (International Organization for Standardization, Geneva, Switzerland, 2011) pp. 3.



Elham Khoshbin received her MSc degree in mechatronics engineering from Arak university in 2016. She is currently a PhD student at UQAC. Her research interests include human–robot interaction, control of cable-driven parallel robots, and reconfigurable parallel robots.



Khaled Youssef received the PhD degree from university of Quebec at Chicoutimi. His research activity focuses on multi-body dynamics, robotics, and linear and nonlinear optimization. He is currently a mechanical engineer at Metfab since 2019.



Ramy Meziane received a degree in electrical engineering (2008) and M.Sc. in Automatic Robotics (2010) from University of Science and Technology (USTHB) Algiers, Algeria. He received also another M.Eng. (Master) in real-time system engineering (2012) from Paul Sabatier University, Toulouse – France, and PhD degree in engineering from University of Quebec at Chicoutimi – Canada in 2018. Since April 2021, he has been with National Research Council Canada, where he is a Research officer. Dr. Meziane is also with Sept-iles college (ITMI) as researcher and Adjunct Professor at University of Quebec at Chicoutimi (LAR.i). His research interests are related to collaborative robotics and cyber-physical system.



Martin J.-D. Otis received the MSc degree in electrical engineering from University of Sherbrooke, Sherbrooke, QC, Canada, in 2004 (as a member of GRAMS in the Department of Electrical and Computer Engineering), and the PhD degree in electrical engineering and robotics from Laval University, Ville de Québec, QC, Canada, in 2009 (as a member of CVSL in the Department of Electrical, Computer Engineering and Robotic Laboratory). He is professor at University of Quebec at Chicoutimi, (2010) and is the LAR.i Director (2013); he is a member of ReSMIQ strategic network (FRQ-NT), research Center CISD and RISUQ network. He was a Post-Doctoral Fellow at Centre for Intelligent Machines, McGill University, Montréal, QC, Canada, in 2010. His research activity focuses on the design of high-performance industrial command and diagnosis, robot control, and system interaction.